

Comparison of remote sensing approaches for detection of peatland drainage in Scotland

Artz, R. R.E., Donaldson-Selby, G., Poggio, L., Donnelly, D., and Aitkenhead, M.J.

The James Hutton Institute; April, 2017.

Summary

Peatland drainage in Scotland has been carried out for over a century, to prepare peatland for afforestation, agricultural or grouse moorland use. Drainage leads to peatland degradation and carbon release, in the form of Greenhouse Gas (GHG) emissions and the release of carbon into waterways. There are few records remaining of where drainage has taken place in Scotland, although this information is vital to enable accurate emissions accounting in the UK GHG Inventory and to assess priority areas to fulfil the ambitious peatland restoration and rewetting targets in the Climate Change Plan.

A first pilot study was undertaken in 2016 to explore the use of earth observations (EO) to detect drains. Here we have extended the modelling approach used in the pilot study, using five different methods to perform mapping of peat drains.

Key findings

- Digitisation of the drainage ditches on peat soils, and classification into 3 drainage categories, was very successful although the cost of manual digitisation at national scale would be prohibitive.
- A very similar level of overall drainage (28.1%) is suggested in comparison with phase 1, which suggests that our sample was sufficient to produce robust statistics of the national level of drainage presence/absence, but does not enable a robust breakdown into drainage categories.
- Automated image detection of drainage ditches shows some promise, although improvement is required.
- Modelling drainage features using Landsat and MODIS satellite data was not very successful, however the detection of undrained areas showed some promise.
- These findings suggest that substantial additional effort would be required. Modelling peatland drainage using EO data sources alone appears to be limited in scope to detecting drained *versus* non-drained areas.
- As the UK GHG Inventory requires both knowledge of the area/location of drained peatlands and the density of drains in order to calculate the net emissions, a layered approach to assessing drainage in peatlands would likely be the most cost-effective way to create national scale coverage.
- In addition, our robust estimate of the proportion of drained peatland (28% of the total peatland area) makes a calculation of the effort required to produce such a layered approach more feasible.

Conclusions and Recommendations

We can conclude that the additional digitisation of drainage channels has resulted in a robust estimate of peatland drainage across Scotland; however the modelling efforts to produce a map of drained peatland locations have not improved with the additional effort. This is most likely due to the resolution of the input data as well as the EO data sources used in this project. However, a layered approach looks to be feasible as non-drained areas can likely be

detected using modelling with EO data sources, followed by the use of automated image detection of the drains in the remaining 28% of the peatland area. We recommend that:

1. Further modelling efforts should make use of finer resolution input data (<100 m) to reduce the effects of the mixing of drainage channels with other drainage features in the same input cell. The use of higher resolution optical and other EO data (e.g. Sentinel-2) could further improve sensitivity of the models.
2. Further improvements could be made by using a time series of EO data rather than median or single image sources as this information could make use of the differential response of the surface moisture through time in drained and undrained areas.
3. Automated image detection could be further improved by iterative steps to remove other features (such as fences and animal tracks) and review of the assumptions on linearity of the drains.

Introduction

Knowing where peat is drained is vital to informing peatland restoration and rewetting. In addition, there are ongoing modifications to the UK Greenhouse Gas Inventory to better represent the emissions from peatlands, both in their drained state, and to accurately account for any emissions abatement represented by rewetting activities. The currently proposed methodology for inclusion of peatlands and their emissions in the UK GHG Inventory would require spatially explicit data on both the locations of drained peatlands, and the density of drains within these areas. The latter is required primarily for the accurate calculation of methane emissions from drains, as both the default Tier 1 methodology as well as the proposed Tier 2 method require information on the proportion of the total area occupied by drains. Farm drainage records, including those for drainage of upland and lowland peatlands, held by the then Ministry for Agriculture, Fisheries and Food (MAFF), the Department of Agriculture and Fisheries for Scotland (DAFS) and other subsequent government bodies, have been lost, and so there is no consistent data source of peatland drainage locations and intensity across the country. Similarly, although restoration activities that aim to restore the habitat value of these ecosystems have been carried out for more nearly two decades in Scotland, these have not yet been captured in a ready to report format.

Given the highly distributed nature of drainage channels, remote sensing was considered a potentially useful tool for mapping the amount of drainage (and potentially restoration efforts) spatially across Scotland. A pilot study conducted by Aitkenhead et al. (2016) concluded that there was significant potential in this approach, but that most likely the sampling had been too limited to detect drainage accurately.

Robertson (1981) gave examples of using remote sensing to map peatland extent and characteristics, along with Stove (1984) and Pala (1984) who demonstrated the effectiveness of remote sensing for peatland class mapping. These works, and those of Stove & Hulme (1980) and Stove & Robertson (1979) used Landsat imagery with a resolution of 30 metres or greater. At this resolution, it is impossible to discriminate small linear features such as drains, fences or narrow tracks. However, Landsat data continues to be useful for peat class mapping due to its ability to provide imagery covering a large spatial extent in a single scene (e.g. Brown et al., 2007).

The use of multitemporal remote sensing has potential for demonstrating changes in peatland characteristics and land cover (e.g. Leine, 1998). Hyperspectral remote sensing has also proved useful for measurement of peat composition characteristics such as moisture content, cellulose and lignin (McMorrow et al., 2004). Wijedasa et al. (2012) showed that even under conditions that are not optimal with missing data from Landsat 7, it is possible to produce composite imagery that provides a near-continuous time series of imagery for changing environments such as peat swamps. This is potentially useful for comparing peatland surface moisture and vegetation characteristics pre- and post-drainage and rewetting, and has been demonstrated as useful for monitoring the impacts and recovery from fires (Segah et al., 2010).

Identification of linear features within remote sensing imagery can be achieved in a number of ways, including the Hough transform (Karnieli et al., 1996) and wedgelet decomposition (Niu et al., 2007). Other methods for detecting edges in high-resolution imagery include Gabor filters and 2D Fourier transforms (Zhao et al., 2013). Detection of edges in peatland environment can also include other morphological measurements relying on shape or edge/area ratios (e.g. Sjöberg et al., 2013). Detection of linear features can be automated to a certain extent (e.g. Pirasteh et al., 2013) but does require tuning to the specific imagery and features of interest. Edges of small lakes or other features within peatland environments requires an understanding of the relevant features and how they are produced (Sannel et al., 2010). Linear features that are small and fragmented are particularly difficult to detect when their spatial scale is similar to that of the remote sensing imagery (Lechner et al., 2009).

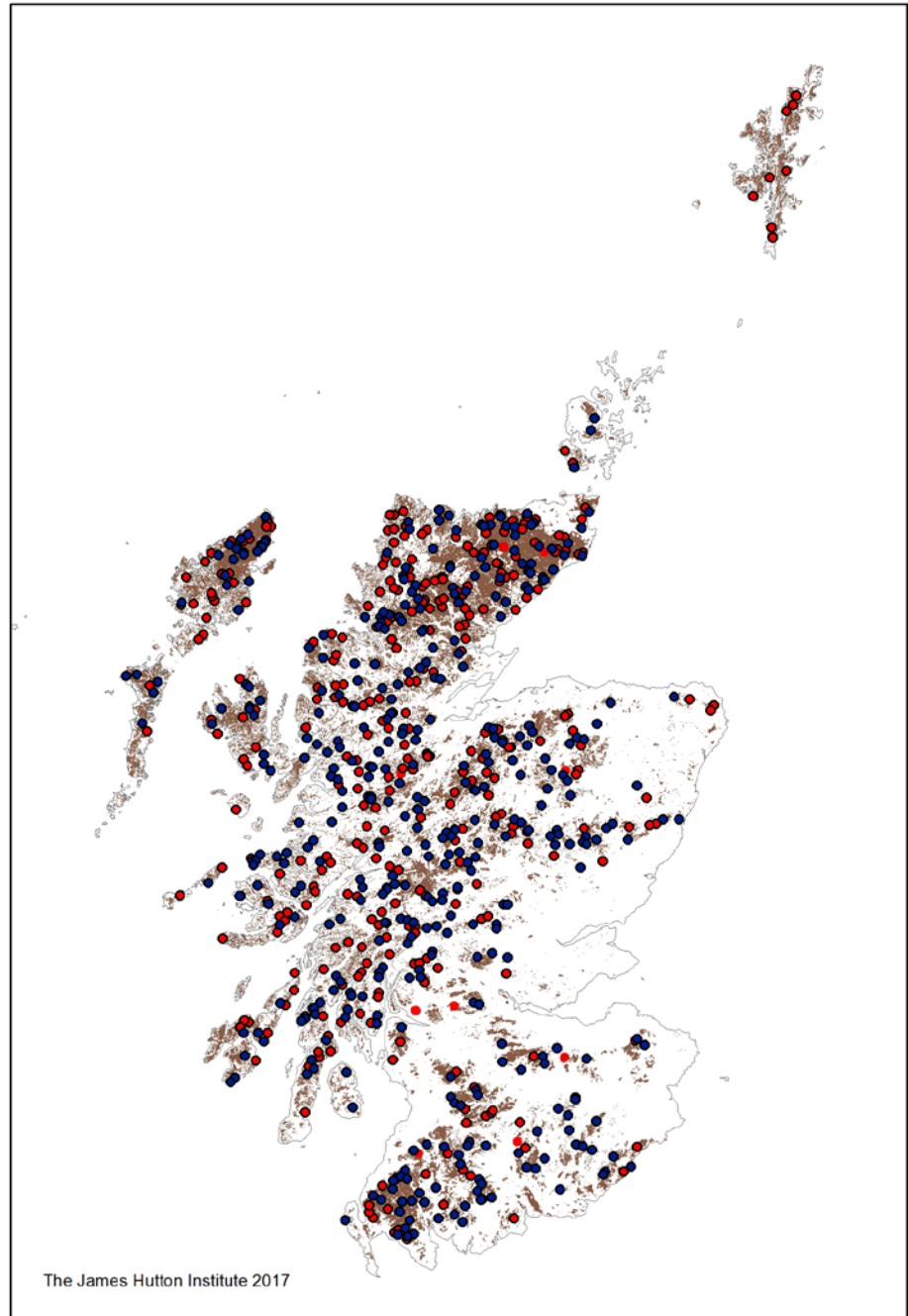
In this project, we attempted to improve on the modelling efforts made in a previous pilot study (Aitkenhead et al., 2016) to detect drainage features. This project more than doubled the available ground truthing data for modelling of peat drains, and further enhanced the available data by identifying cover of other features on the ground that could also contribute to drainage effects, such as erosion gullies, former domestic peat cuttings and standing and felled forestry on peat soil. In addition, a new algorithm was developed to attempt the automated detection of drains in high resolution aerial photography.

Methods

GetMapping imagery

High-resolution aerial photography was provided through licence with GetMapping. This imagery provides full coverage of Scotland at a spatial resolution of 0.25 m, with a rolling programme of flights guaranteeing imagery is no more than 5 years old (and is usually less than 3 years old). This imagery is provided for scientific use under licence covered by RESAS. Only the visible range imagery was used for the purpose of this project. For this phase of the project, total of 400 georeferenced points across Scottish peatland were randomly generated using conditioned Latin hypercube sampling (Minasny and McBratney, 2006) and used as centroids for 500m x 500m blocks. These sites were selected using a stratification approach designed to ensure that there was equal representation across different elevation, easting, northing and climate ranges. The underlying maps used were a combination of the LCS88 and the Scottish Soil Map at 1:250,000 scale. Both datasets were used due to the low spatial resolution of the Scottish Soil Map and the lack of spatial information on the location of peat within mixed soil polygons. The corresponding 400 image blocks were extracted from the GetMapping imagery. Figure 1 shows the location of these image blocks relative to the 338 Phase 1 (Aitkenhead et al., 2016) blocks. For a proportion of these images, there were areas within each 500 m block that were not classed as peat in the Scottish Soil Map as of the centroids of these sites fell onto polygons with relatively small pockets of peat or were on the edges of peatland areas.

Figure 1. Distribution of the 500 m Phase 1 (red, n=338, Aitkenhead et al., 2016) and Phase 2 (blue, n=400, this work) input blocks. Areas shown in brown are discrete peat areas as modelled using a combination of the Scottish Soils Map at 1:250,000 combined with the peat areas from the British Geological Survey (Digimap v7) at 1:50,000, where modelled peat areas within remaining mixed soil polygons were limited to areas with <15% slope as based on the 5 m Ordnance Survey DTM. The circles show the centroid location of the input blocks.



Manual interpretation

Two Phase 2 blocks where only a very small fraction of the 500 m block fell on peat were excluded, as was one phase 2 block that partially overlapped with an existing block from phase 1 of this work (Aitkenhead et al., 2016). Each of the remaining 735 blocks was superimposed over 25 cm GetMapping aerial imagery and manually examined for signs of peatland drainage. Blocks were graded as 0, 1, 2 or 3, where 0 meant that there no peatland drains in the block while blocks graded as 3 were completely drained by peatland drains alone. Additionally, the blocks were also separately graded by any additional features that could contribute to drainage effects as the EO data would observe them in each 500 m block (e.g. different vegetation types, bare peat). This resulted in a matrix of drainage classes as shown in Table 1. The visual examination process was carried out iteratively and by two people working independently at first. Their results were later compared, to ensure that agreement was reached on the score given to each block and that the scoring was as accurate as possible.

The resulting dataset of 735 graded blocks was produced as input data for modelling, with 10 potential classes for each observed combination of drainage channel intensity x other draining features (Table 1). However, due to the very low number of observations in some of these classes, for example, only 9 observations in the class containing grade 2 drainage channels and grade 3 other features, some classes were grouped together for the MODIS modelling, resulting in 6 classes.

Table 1. Counts of drained and non-drained peatland blocks. These data were grouped into classes as follows: Class 1= not drained (no drains, no other drainage features, yellow), Class 2 = no drains but other drainage features present (orange), Class 3 = low number of drains, low number of other drainage features (light blue), Class 4 = low or medium number of drains, but a medium-large proportion of other drainage features (dark blue), Class 5 = medium number of drains and medium other drainage features (green), Class 6 = high density of drainage channels, no or only sporadic other drainage features (black).

		Drains alone			
		0	1	2	3
Other draining features	0	192	0	0	38
	1	160	68	0	0
	2	90	15	68	0
	3	84	11	9	0

Manual digitisation

In this phase of the study, 151 of the drained GetMapping image blocks were processed to produce a manual digitisation of all peat drainage channels. All of the 38 grade 3 blocks, most of the 68+9 grade 2 blocks and some grade 1 blocks were used for manual digitisation of the ditches. The digitisation was carried out by eye using GlobalMapper v18.1, by an operator trained in distinguishing peat drainage channels from other landscape features (e.g. animal tracks, fence lines) and from other types of drainage channels (e.g. erosion gullies, peat cuttings). Each channel network was digitised as a polyline feature, and the layer then converted to a raster dataset with spatial resolution of 0.25 metres. Feature width was set at this spatial resolution, regardless of the actual drainage channel width.

All peatland drains identified in each aerial imagery block were digitised and attributed with respect to the year of photography, drain width and (where possible) spacing. Where appropriate, attributes were also added indicating erosion, any already completed restoration efforts (i.e. drain blocking and associated created pools, attributing pool spacing and pool size), standing forestry and peat cuttings. Simulated elevation data files for use in satellite image recognition of peatland drains were generated from combined 500m x 500m blocks and digitised drains, where the 500m x 500m blocks were assigned a height of 255 and the drained areas a height of 0. These 'heights' are simply a means to provide coding for a difference in elevation between the areas that the drains occupy and the surface of the

peat. There are no units and the numbers are only required to provide a contrast for modelling, they do not represent actual height differences between drains and adjacent surfaces.

Automated aerial imagery interpretation

Each of the image blocks identified as having peat drainage was passed through an image analysis processing chain designed to detect narrow, straight features. This included edge detection at a number of spatial scales, and the elimination of edge features that were either too broad (wider than 2 metres) or that occurred at the boundaries between areas of visibly different land use/cover types. Drainage channel detection was carried out using a stochastic search that selected random pairs of points and evaluated the probability of there being a straight drainage channel between them. This allowed for 'partial' channels or channels with slight curvature to be identified.

Landsat data

Full coverage of Scotland from Landsat scenes was captured from the USGS data download service. These scenes each occupy an area of land approximately 180 x 180 km, and therefore a minimum of 9 scenes need to be stitched together to provide full cover of Scotland. None of those 9 scenes was completely cloud-free, and so in practice it required 15 scenes that were stitched together (omitting areas with dense cloud cover) to provide an (almost) cloud-free image of Scotland. For each of the drained blocks, the Landsat scene pixels were extracted (each Landsat pixel is 30 metres across). These pixels' digital values at 8 wavelength ranges were then statistically compared to the proportion of drainage channels in each. This proportion was calculated by dividing the number of drainage channel pixels in the high-resolution aerial photography by the total number of high-res pixels for each 30 metre Landsat pixel area. There were no clear correlations between individual bands or band combinations and drainage channel density per Landsat pixel. A neural network model was therefore applied in an attempt to determine any more complex relationships that may exist between drainage density and spectral response from Landsat data. The Landsat-based modelling was carried out using a categorization of the image blocks that included both artificial and natural drainage features. This effectively combined multiple classes from Table 1 into 4 categories (1+2, 3+parts of 4, parts of 4+5, 6). The effect of this was to confuse the impacts of natural and artificial drainage features on the spectral reflectance, reducing the model effectiveness. This part of the work was carried out before it was realized that it was necessary to separate out the six classes as specified in Table 6, and by the time the mistake had been detected there was no time remaining to repeat the work. A re-run of this component combined with the suggested model design improvements in the Discussion may improve the accuracy of Landsat-based evaluation of artificial drainage.

MODIS data

The median of MODIS data for 12 years (2000-2011) were used, with clouds gaps were filled using the method described in Poggio et al (2012). A randomForest approach was used with the following covariates: a) elevation, b) surface with xy tensor created using a Generalized Additive Model (GAM, Wood, 2006) and c. MODIS surfaces (as median of 2002 to 2011) for: i. EVI and its seasonality trends, ii. Snow index (Poggio, Gimona, 2015), iii. NDWI, iv. Primary productivity, and v. Land Surface temperatures. The validation statistics were calculated on an out-of-sample set obtained by randomly sampling 30% of the locations from the dataset. This split was repeated 100 times and the statistics averaged over the iterations.

Results

Manual interpretation of aerial photography

For the image blocks scored as low (but not zero) artificial drainage channel density, the mean density of image pixels assigned to drains was 0.15%. For images scored as medium artificial drainage channel density, this value was 0.25%, and for images scored as high artificial drainage channel density it was 1.19%. While these percentages may seem small, it is worth remembering that peatland drainage channels are typically only 0.5 metre across (the width of the Cuthbertson plough used for the majority of older drains) and that they can be between 20 and 100 metres apart even in areas that are targeted for drainage. The drain spacing in areas targeted for forestry plantations can be as low as 3 m but typically it is in the region of 10 m for most upland drainage. In addition, at low and medium density categories, only part of each 500 m block was affected by drainage. The range of drainage pixel density values for each of the three categories was wide, however, with some high values for image blocks scored as 1 (low drainage density) and some low values for blocks scored as 3 (high drainage density). Some error may lie in the human interpretation of the imagery, as the human brain is very effective at filtering out what it perceives as noise. For example, discontinuous (old, overgrown) drains may be perceived by the person grading the images as continuous (the eye fills in the missing part). However, it is also probably largely due to the fact that the visual-based scoring made the assessment based on the area of drained peat within the image as well as the perceived density of these drains. To the person grading the images, the area occupied by dense drainage in one part of the image may be perceived as higher grade drainage than if there were widely spaced drains across an entire image. So an image block with very high density of drains for only a small part of the image will have received a low score, while the mean density of drains for that block could be relatively high (Figure 2).

Automated interpretation of drainage channels in aerial photography

For the automated drainage channel detection, the success of the method applied varied greatly across the images. For some images such as the series shown in Figure 3, the original images had clear, fairly straight drainage channels that showed up clearly in the edge detection output imagery and reasonably well in the subsequent drainage channel detection. For other images, the drainage channels were less well detected and there were many instances of false positives in some images. The parameterisation of the final drainage channel detection appears to be the controlling factor in the success of this method, with several parameters being adjustable and optimal values required in order to make the method work for all images. This is particularly true during the final edge detection phase of the image analysis, where drains are highlighted and then kept or discarded based on their width, strength and curvature. The examples shown in Figure 3 suggest that the initial assumptions about drain width, strength, continuity and curvature are presently too rigid to allow accurate assessment of drainage channels. However, tests run to relax some of the rules suggested an increase in false positives, as the method starts to pick up other features with similar width such as fence lines, similar curvature such as animal tracks, or simply assigns classification as a presumed drainage channel to noise in the data. Future work in this area would need to focus on improving primarily the image processing chain in order to highlight drainage channels against the often highly complex and fragmented landscape.

Landsat-based modelling

The Landsat 8 imagery was demonstrably capable of identifying undrained, wet peatland areas (not shown). However, we identified a problem very late in the project in that the input data used for the modelling ignored the competing drainage factor attributes, and so only used the 'drains alone' classes rather than the matrix shown in Table 1. Hence the results obtained are using mixed classes. In the case of the undrained areas, it mixed areas without drains and without other drainage feature (i.e. semi-intact peatland) with areas without drains but other drainage features still present (e.g. areas without drains but suffering from various degrees of erosion, peat cutting or under grassland/forestry). Therefore, the modelling would require to be re-run in order to give the appropriate output statistics. This problem was unfortunately identified too late in the reporting period to be rectified within the limit of the project.

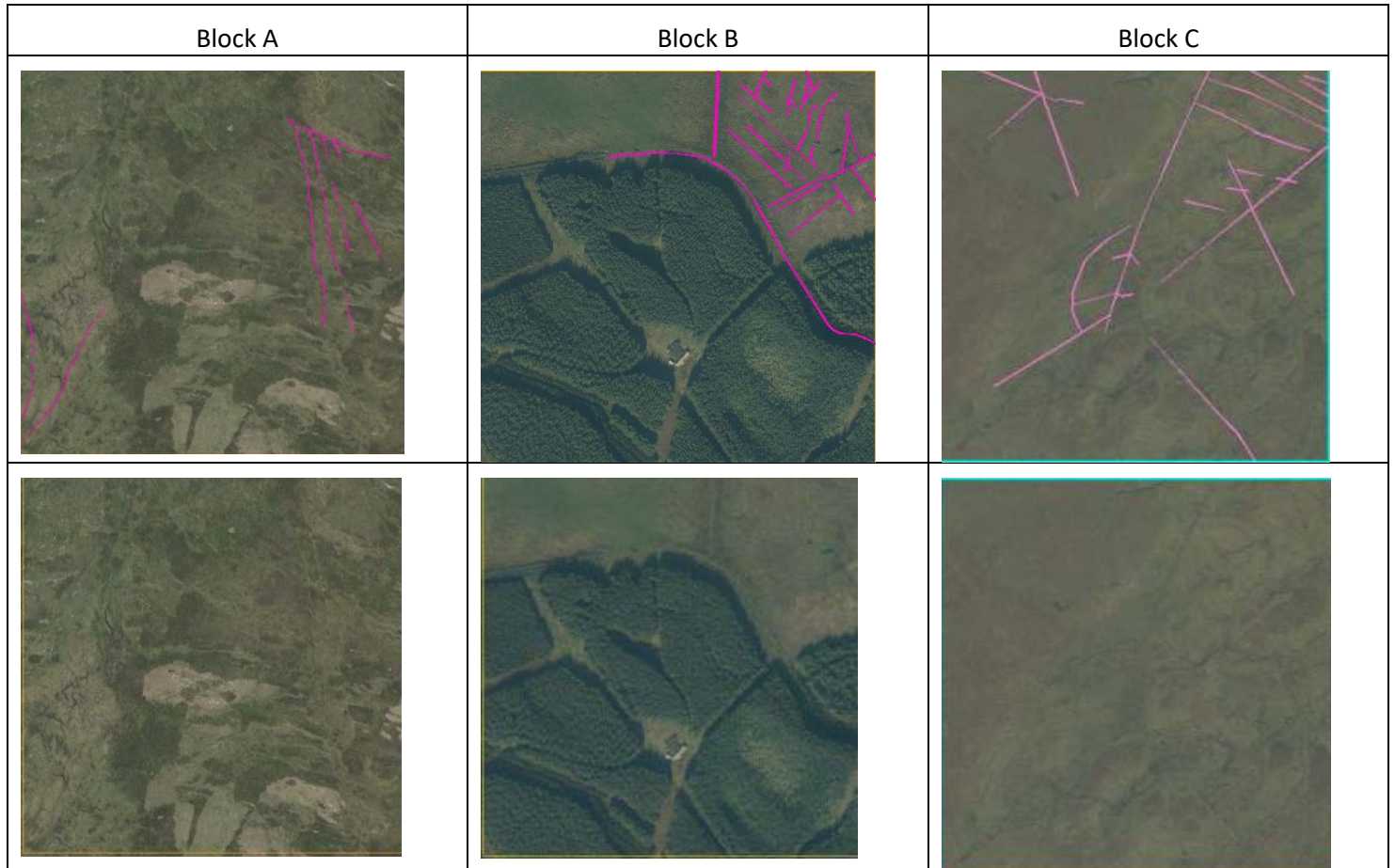


Figure 2. Examples of digitized drains (top row) in three grade 2 blocks. The bottom row shows the original image for comparison. The three examples clearly show the heterogeneous distribution of drains within 500 m blocks, with the left most (Block A) and central image (Block B) showing denser drains in an overall smaller area, whereas the block on the right (Block C) contains more widely spaced drains across a wider area.

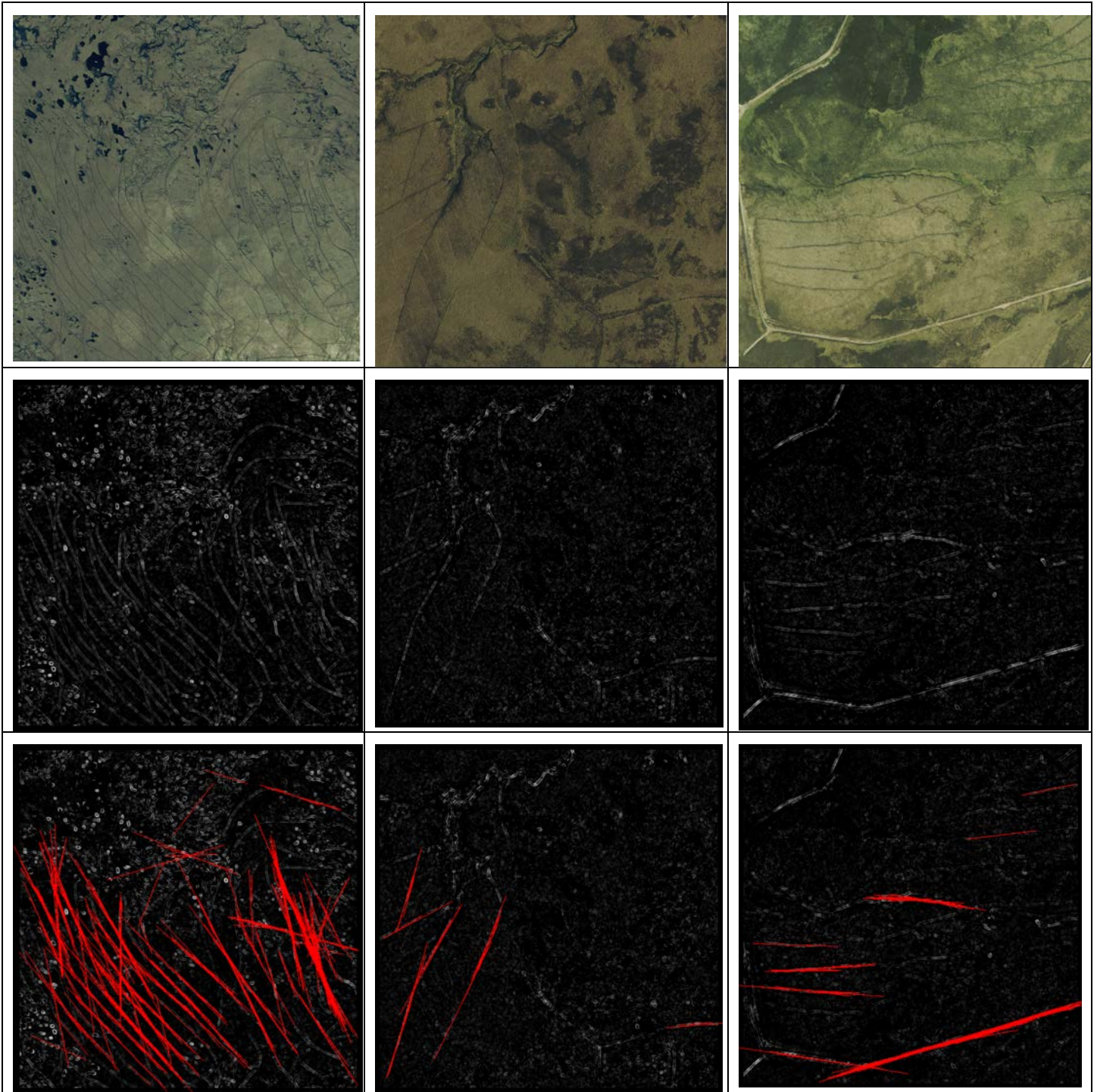


Figure 3. Illustration of the automated drain detection using high resolution aerial photography (top row), clearly showing the location of the drainage ditches. Note the old, overgrown, ditches in the middle block. The middle row shows the raw edge detection images after processing, again with the majority of the ditches visible. The lower row shows the results of the automated discrimination of candidate drainage channels, with locations of the 'drains' in red. This final algorithm clearly requires further improvement (see text); for example, a road is detected as a drain in the far right block.

The modelling approach that used the statistics extracted from the digitized drains directly (i.e. attempted to model the area occupied by a digitized drain in each 30 m Landsat pixel, thereby using the highest resolution available) also did not produce satisfactory results. Very low correlations between individual Landsat bands and drainage channel density within the 30 m Landsat image pixels were seen. None of these correlations gave r^2 values was greater than 0.05. The modelling that included all Landsat bands used to train a neural network gave better estimation abilities, with an r^2 of 0.14. This is still not a good modelling accuracy, and we believe the primary reason for this is that large variations in spectral characteristics across the multiple image blocks are masking the small spectral signature of the effects of drainage. Across the whole of the Scottish peatlands, there are not only multiple competing features contributing to drainage effects, there are also further differences in vegetation structure between e.g. hyperoceanic blanket bogs and lowland raised bogs as well as large altitudinal gradients with consequent differences in the length, onset and end of the growing season, which in turn affects the spectral signature at the time point chosen for the satellite images. There is another complicating factor in that the altitudinal gradient also likely affects the presence and density of some of the competing drainage features, as localised peat cutting is more likely to occur in lowland areas (nearer human populations), whereas e.g. erosion is more pronounced at greater altitude and latitude. Even averaging across several time points in EO data would not negate this effect, as the overall productivity of different peatlands differs greatly across Scotland and the underlying altitudinal and latitudinal gradient of the competing features would still present a challenge.

MODIS-based modelling

The MODIS-based model based on the original 6 input classes (Table 1) also proved to be low in predictive ability (Table 2). The best model performance was for the prediction of other drainage features, rather than the drains themselves. For example, Class 5 (medium number of drains and medium other drainage features) is accurately predicted approximately 1/3 out of 100 iterations of model runs, whilst Class 6 (large number of drains) is never predicted correctly. Class 1 (no drains, no other drainage features) could only be correctly predicted 6.1% of the time over 100 iterations, whilst the model placed observed Class 1 blocks primarily into Class 5 (medium number of drains and medium other drainage features). This tendency of the model to place blocks into Class 5 regardless of their actual class membership is evident across Table 2. As for the Landsat-based modelling, we believe that the inherent differences in productivity and underlying altitudinal/latitudinal differences in land use of peatlands across Scotland are the primary factors contributing to the poor predictive model outputs. One possible alternative explanation, however, was that the model was constrained by the low number of observations per class.

Table 2. Misclassification table using all 6 classes over 100 iterations of cross-validation. Figures in this Table should be read as the proportion of predicted classes matching an observed class over 100 iterations. Classes highlighted in green are the figures for correctly attributing observed classes, i.e. the model correctly interpreted class 5 input blocks as class 5 32.5% of the time over 100 iterations, but was completely unable to correctly predict class 6. The mean kappa statistic is 0.0233433, the maximum over the iterations is 0.1639235.

	1	2	3	4	5	6
1	0.061	0.014	0.009	0.011	0.090	0.006
2	0.006	0.002	0.005	0.002	0.014	0.001
3	0.007	0.008	0.006	0.003	0.014	0.002
4	0.003	0.002	0.002	0.000	0.002	0.000
5	0.188	0.067	0.066	0.039	0.325	0.033
6	0.002	0.001	0.002	0.001	0.005	0.000

In order to test whether the poor model performance was primarily due to the low number of observations in some of the classes, we produced a more condensed classification as per Table 3 by combining all classes with intermediate drainage channels and/or competing features that could produce drainage effects on the ground. This improved the model performance slightly, however not to a level that could be considered adequate in order to be used as a predictive model (Table 4). Although the end points (undrained or fully drained) were predicted correctly a little better than in the 6-class model, the effect observed in the original model, i.e. a strong tendency to classify the majority of data as heavily drained by other features but only containing a small to medium number of drainage channels, persisted.

Table 3. Condensed classification to increase group size. Class 1= not drained (yellow), Class 2 = no drains but other drainage features present (green), Class 3 = low or medium number of drains, but also a large proportion of other drainage features (blue), Class 4 = high density of drainage channels, no or only sporadic other drainage features (black).

		Drains alone			
		0	1	2	3
Other draining features	0	192	0	0	38
	1	160	68	0	0
	2	90	15	68	0
	3	84	11	9	0

Table 4. Misclassification table for the condensed classification-based model as per Table 3 over 100 iteration of cross-validation. The mean kappa statistics is 0.1259082, the maximum over the iterations is 0.2760191.

	1	2	3	4
1	0.064	0.009	0.088	0.025
2	0.002	0.000	0.001	0.001
3	0.166	0.026	0.291	0.123
4	0.031	0.016	0.071	0.085

For both the Landsat and MODIS-based modelling, the poor predictive capacity of the models also suggests that there is likely some further internal variation within the 500 m images that causes such poor performance. We therefore manually re-inspected 8 random examples of the grade 3 drained images that had been classed to contain no other draining features (Figure 4). It is clear in even just these example images that there are a substantial number of other features in these image blocks that could confuse a modelling effort. For example, in the lower row, the image second from the left, and the image furthest right, both contain roads. In addition, both the furthest left and furthest right image in the lower row contain water bodies within the 500 m block. In the upper row, substantial variation in the sharpness of the drains can be seen, which likely represents their age and whether they have overgrown and infilled to a certain extent. In addition, even in this small selection out of the 38 blocks graded as Class 6, there are substantial differences in the mean altitude (causing differences in vegetation growth due to temperature constraints), slope (causing differences in growth due to local variation in daylight) and the likely land use for which the drainage occurred (Table 5). All of these factors cause significant variation in what ‘the satellite sees’.

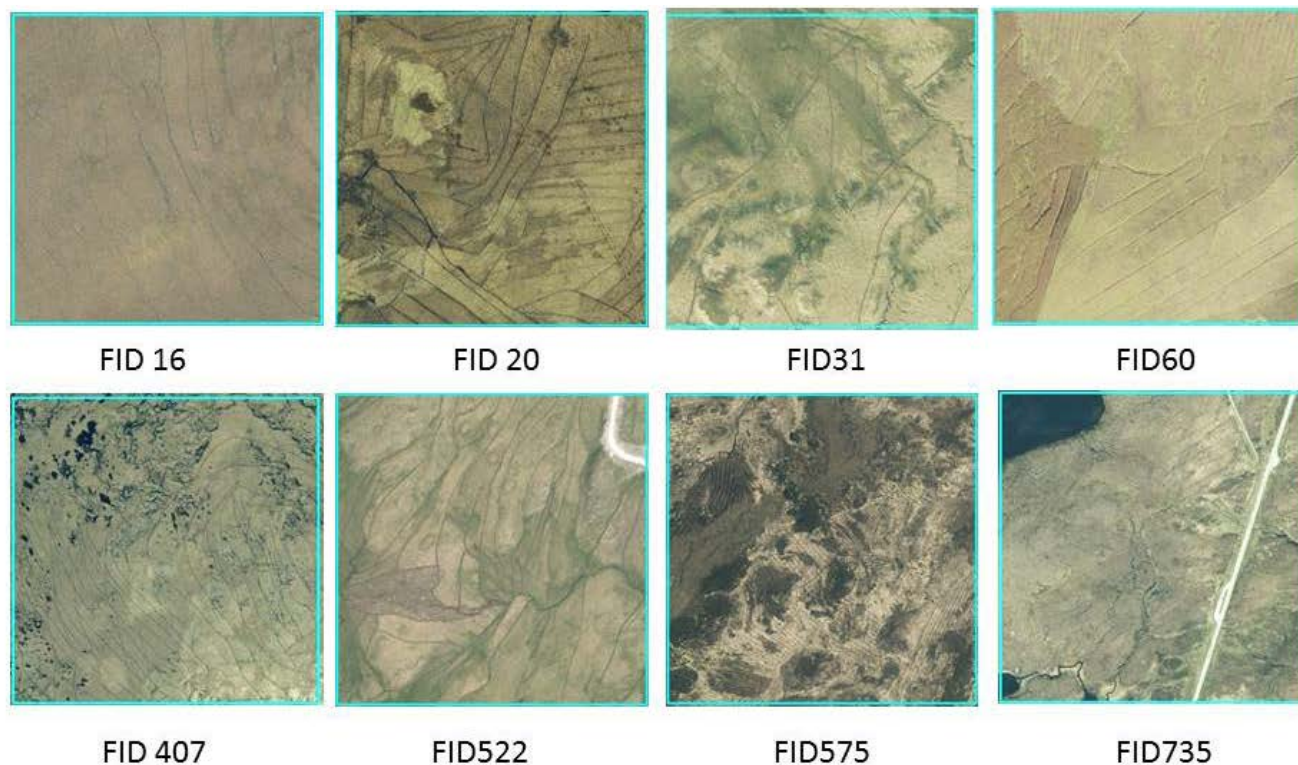


Figure 4. Random example blocks out of the class 6 category (fully drained by drainage channels, no other draining features).

Table 5. Mean altitude, slope (low = below 20 m across image, medium = below 50 m across image, high = (> 50 m across image) and primary land use for which the peatland was drained (interpreted from image block in conjunction with areas in immediate vicinity).

Block FID	Mean altitude (m)	Slope class and primary surface attribute
16	140	Low (slightly convex)
20	200	Medium (sloping to SW)
31	470	High (sloping to NW)
60	250	High (sloping to NE)
407	320	Medium (concave)
522	380	Medium (sloping to S)
735	240	Medium (concave E-W)

Discussion

Despite the doubling of effort in terms of input data, our efforts to detect peatland drainage directly from EO and aerial photography sources have only been mildly successful. Detecting peatland drains directly from satellite data sources, in particular, was not successful. This approach does not seem to have a precedent as we were unable to find any published material of other attempts to which we could compare our methodology. We are aware of a recently completed research project by Rezatec for Scottish Water, which modelled peatland condition inclusive of linear features such as drains, using Sentinel-1 and 2 data (http://www.rezatec.com/wp-content/uploads/Rezatec_DataSheet_Peat_Digital.pdf). However, there is no published report on this work available in the public domain at present and therefore we are unable to compare the approaches.

Our experiences with Landsat and MODIS satellite data have shown predictive modelling of peatland drainage to be very complex, as the model quality depends on the level of heterogeneity within the factors causing drainage effects in the input data as well as the level of response from drainage features against the competing variability in the image caused by other factors such as inherent differences in vegetation productivity due to the location of the site. The former issue could be improved by re-classification of the existing images at higher resolution, and taking additional steps to remove blocks containing non-peatland features such as roads, water bodies, buildings, rocks, or snow. Such an improved classification scheme could take the form of the matrix in Figure 5, or an even more complex coding system that disentangles the individual competing features. The problem that then arises is one of a requirement of a vastly higher sampling effort, as an increase in the number of classes to be predicted needs to be matched by an appropriate increase in the observations per class.

		Drains (number in image)		
		0	1	>1
Other draining features	0	1	3	5
	1	2	4	6

Figure 5. Classification scheme for coding higher resolution input data, using 999 for blocks with non-peatland features (e.g. roads, buildings, other soil types, water).

We reclassified two of the class 6 blocks (fully drained) out of the 735 input blocks at 100 m resolution (Figure 6). This figure shows just how much variability within the input blocks is masked within the single classification at 500 m. For example, even within the relatively evenly distributed drains in the image on the left, there was sufficient variation in the drainage density, but also in the presence or absence of minor erosion features, to create a much more complex input dataset at 100 m resolution. In more structurally complex 500 m blocks, for example the image on the right, the 500 m block includes not only drained peatland, but also two lochs, several streams, and a road. In our 500 m resolution MODIS model using this input image, any variability introduced by these additional features is neither captured in the coding, nor the EO data resolution, and hence contributes to the low predictive capacity of the model. Hence, any future attempts should utilise higher resolution EO data sources.

Another potential source of error is that some of the 500 m blocks were likely not entirely covered by peat soil. The model based on the 1:250,000 Soils of Scotland map used for this project includes a series of assumptions over where peat occurs and is not spatially accurate within some of the mixed soil:peat polygons. Hence, the models may be attempting to model peat drainage on soil that is in reality not all peat within a 500 m block. This may be reflected in differences in vegetation at local scale which we would not be able to detect as an error term in the model.

Some of the above issues cannot be resolved, for example, there is no map of peat soil for Scotland that is known to be accurate at 100 m or below. There are, however, some other improvements that could be attempted, by using the characteristic that peatland drainage lowers soil surface moisture and water table (Holden et al., 2007). Wilson et al (2010) suggested that there was a 2 m zone either side of drains where surface moisture is affected in drained Welsh peatlands, and water table effects extended to 5 m. This may suggest that the water table and/or surface moisture in drained areas recovers more slowly after rainfall, and is prone to faster drawdown in drought periods, compared to non-drained areas. Hence, it would be useful to investigate whether time series of EO data could distinguish better between drained and undrained areas as there could be a larger amplitude through time in the surface moisture response, and possibly also the vegetation structure.

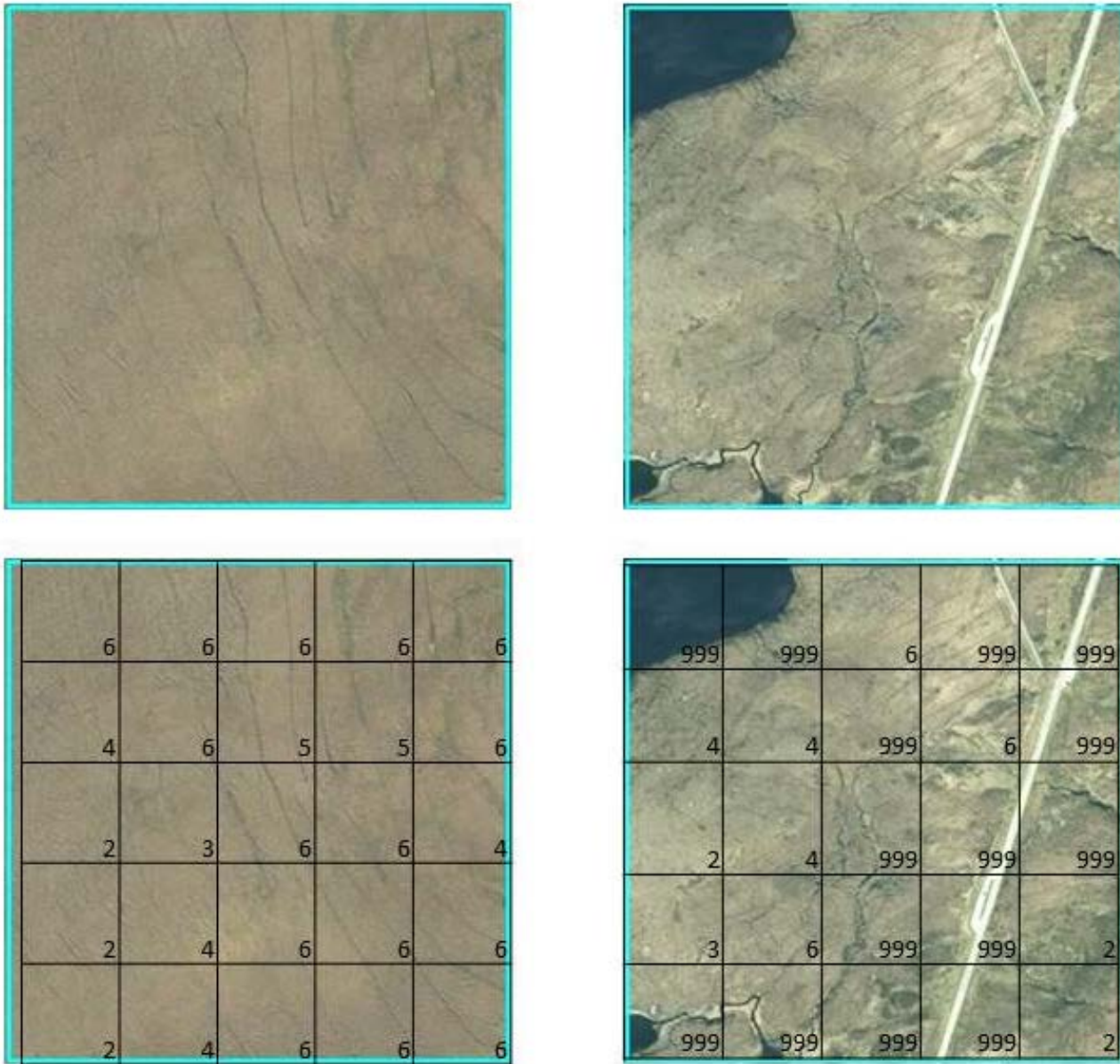


Figure 6. Subclassification of two example 500 m blocks into 100 m input data, using the enhanced classification matrix in Figure 5.

The detection of actual drains as attempted using automated image analysis was only partially successful in that the edge detection algorithm produces promising textural data where the drains are visualised quite clearly; however the final classification step clearly requires further improvement. Object based image analysis on aerial photography was very successfully used by Connolly and Holden (2017) to detect drains in a 68 km² pilot area in the west of Ireland, using GeoEye high resolution aerial imagery (similar in resolution to our GetMapping dataset). Using Feature Analyst™ software, the authors used similar initial assumptions to classify potential drainage features, however their approach is superior in that the software used utilises further iterative steps during which linear features that have been initially classed as drains but are not drainage channels (e.g. fences, steep hillside edges, shadows and streams) can be excluded using further manual training (using the iterative correction function). In addition, their chosen area of interest showed much denser and more straightforwardly linear drainage channels than the majority of our Scottish sites, as their area was primary drained for peat extraction. It is likely that these factors (limited area, strongly linear and dense drains) present fewer difficulties than the typically more curved and often discontinuous hill drains that cover much of the Scottish peatlands. However, their example is encouraging and further refinement of the edge detection algorithms for Scottish peat drains can be envisaged.

Finally, Connolly and Holden's (2017) costings breakdown suggests a budget of just under €5,000 for object based image analysis based methods for their 68 km² pilot area, against a € 10-11,000 budget for the same area for manual digitisation or ground surveying. Scaling these costs to the Scottish peatland area would equate to ca. € 73 per km², or ca. £1.5 mi, in order to use this rather more sophisticated method of modelling drainage channel locations. In contrast, full manual digitisation or ground surveying would likely run into the order of £3.5 mi. Clearly these options are not cost effective for mapping peatland drainage in Scotland. Hence, development of a multi-layered approach that uses the strengths of the various available EO data sources and image analysis of high resolution aerial photography would be advisable, in order to be able to fulfil the mapping obligations for drained peatlands for the UK Greenhouse Gas Inventory. However, it is clear that a substantially higher effort than the initial pilot study of Aitkenhead et. al., (2016) and the present work is required to fulfil these data needs. Running improved edge detection algorithms for 28% of the Scottish land area would equate to an approximate cost of £40,880 alone, according to the cost estimates in in Connolly and Holden (2017). This cost needs to be considered in addition to the likely staff and computing cost for modelling of non-drained *versus* drained areas. However, we still believe that a layered approach could be a very cost-effective way to accurately estimate the area occupied by drained peatlands as well as estimating the density of drains for inclusion in the UK GHG Inventory.

Recommendations

Despite the limited success of the modelling approach used in this study, we believe that further improvements could be made. It is not financially viable to construct a database of all drainage channels across the Scottish peatlands using manual digitisation. It was possible to detect areas that were not drained with some degree of accuracy in the Landsat-based assessments, and hence a nested approach to detecting drains is likely feasible. This should consider using the full temporal capability of EO datasets, as well as input data at higher resolution. Areas modelled to be drained (estimated at 28% of the peatland area on the basis of the present work) could be candidate sites for automated image classification based on edge detection methodology, if the latter were to use better classification algorithms.

1. Improve spatial resolution of input data. The existing 735 image blocks at 500 m could be subsampled into 100 m or even higher resolution (i.e. up to Sentinel-2 resolution) cells to provide data with less interference from competing drainage features such as forestry, peat cuttings and erosion channels. Such subclassification could also be used to exclude areas with water, non-peat soils or roads. This would require some additional work to repeat the drainage class coding, which we estimate as requiring ca. 120 staff hours (16.2 days).
2. Utilise the full temporal capacity of EO data sources to aid the identification of drainage channels, given the slower response of the water table and surface moisture of drained areas to rainfall, and faster drawdown in drought periods. We could produce estimates of the likely staff and computing requirements on request.
3. Improve the edge detection algorithms further so that the final classification of drainage channels is improved, for example the rules for drain linearity. Iterative steps to exclude false positives (fences, tracks) would likely also be required if the initial rules for drainage channel designation are relaxed.

References

1. Aitkenhead, M., Poggio, L., Donaldson-Selby, G., Gimona, A., Artz, R. (2016) Detection of peatland drainage with remote sensing – a scoping study. http://www.climatexchange.org.uk/files/8314/6582/3733/Detection_of_peatland_drainage_with_remote_sensing_a_scoping_study.pdf
2. Brown, E., Aitkenhead, M.J., Wright, R., Aalders, I.H. (2007) Mapping and classification of peatland on Lewis using Landsat ETM+. *Scottish Geographical Journal* 123(3), 173-192.
3. Connolly, J., Holden, N.M. (2017) Detecting peatland drains with Object based Image Analysis and Geoeye-1 imagery. *Carbon Balance Management* 12:7.
4. Holden, J., Gascoign, M., Basoanko, N.R. (2007) Erosion and natural revegetation associated with surface land drains in upland peatlands. *Earth Surface Process Landf.* 21: 1547-1557.
5. Karnieli, A., Meisels, A., Fisher, L., Arkin, Y. (1996) Automatic extraction and evaluation of geological linear features from digital remote sensing data using a Hough transform. *Photogrammetric Engineering and Remote Sensing* 62(5), 525-531.
6. Lechner, A.M. Stein, A., Jones, S.D., Ferwerda, J.G. (2009) Remote sensing of small and linear features: Quantifying the effects of patch size and length, grid position and detectability on land cover mapping. *Remote Sensing of Environment* 113(10), 2194-2204. DOI 10.1016/j.rse.2009.06.002.
7. Leine, M. (1998) Multitemporal analysis of tree cover changes on a southern Swedish raised peat bog. *Proceedings of the 27th International Symposium on Remote Sensing of Environment*, 692-697.
8. McMorrow, J.M., Cutler, M.E.J., Evans, M.G., Al-Roichdi, A. (2004) Hyperspectral indices for characterizing upland peat composition. *International Journal of Remote Sensing* 25(2), 313-325. DOI 10.1080/0143116031000117065.
9. Minasny, B., McBratney, A.B. (2006) A conditioned Latin hypercube method for sampling in the presence of ancillary information. *Computers & Geosciences* 32: 1378-1388.
10. Niu, R., Me, X., Zhang L.-P., Li P.-X. (2007) TI Linear features extraction from remote sensing image based on wedgelet decomposition. In (Ed.) Zhang, Y.J., *Proceedings of the Fourth International Conference on Image and Graphics*, Chengdu, China, 508-512. DOI 10.1109/ICIG.2007.37.
11. Pala, S. (1984) A LANDSAT-based method for the survey and inventory of peat resources over extensive regions. In (Ed.) Robertson, R.A., *Remote sensing in peat and terrain resource surveys*, 156-168. The Macaulay Institute, 1984.
12. Pirasteh, S., Pradhan, B., Safari, H.O., Ramli, M.F. (2013) Coupling of DEM and remote-sensing-based approaches for semi-automated detection of regional geostructural features in Zagros mountain, Iran. *Arabian Journal of Geosciences* 6(1), 91-99. DOI 10.1007/s12517-011-0361-0.
13. Poggio, L., Gimona, A., Brown, I., (2012). Spatio-temporal MODIS EVI gap filling under cloud cover: an example in Scotland. *ISPRS Journal of Photogrammetry and Remote Sensing* 72, 56-72.
14. Poggio, L. and Gimona, A. (2015). "Downscaling and correction of regional climate models outputs with a hybrid geostatistical approach". *Spatial Statistics* 14: 4-21.
15. Robertson, R.A. (1981) Peat resource survey and utilization in Scotland. In (Ed.) Fuchsman, C.H., *Proceedings of the 1981 International Peat Symposium*, 539-555.
16. Sannel, A., Britta K., Brown, I.A. (2010) High-resolution remote sensing identification of thermokarst lake dynamics in a subarctic peat plateau complex. *Canadian Journal of Remote Sensing* 36(SI), S26-S40.

17. Segah, H., Tani, H., Hirano, T. (2010) Detection of fire impact and vegetation recovery over tropical peat swamp forest by satellite data and ground-based NDVI instrument. *International Journal of Remote Sensing* 31(20), 5297-5314. DOI 10.1080/01431160903302981.
18. Sjoberg, Y., Hugelius, G., Kuhry, P. (2013) Thermokarst Lake Morphometry and Erosion Features in Two Peat Plateau Areas of Northeast European Russia. *Permafrost and Periglacial Processes* 24(1), 75-81. DOI 10.1002/ppp.1762.
19. Stove, G.C. (1984) Improved peatland classification using principal components analysis based on synthetic variables: a remote sensing methodology for peat resource surveys in Scotland. In (Ed.) Robertson, R.A., *Remote sensing in peat and terrain resource surveys*, 75-86. The Macaulay Institute, 1984.
20. Stove, G.C., Hulme, P.D. (1980) Peat resource mapping in Lewis using remote sensing techniques and automated cartography. *International Journal of Remote Sensing* 1(4), 319-344.
21. Stove, G.C., Robertson, R.A. (1979) Remote sensing in peat-resource and land-use survey. *ARC Research Review* 5(1), 21-27.
22. Wijedasa, L.S., Sloan, S., Michelakis, D.G., Clements, G.R. (2012) Overcoming Limitations with Landsat Imagery for Mapping of Peat Swamp Forests in Sundaland. *Remote Sensing* 4(9), 2595-2618. DOI 10.3390/rs4092595.
23. Wilson, L., Wilson, J., Holden, J., Johnstone, I., Armstrong, A., Morris, M. (2010) Recovery of water tables in Welsh blanket bog after drain blocking: discharge rates, time scales and the influence of local conditions. *J Hydrol* 391: 377-386.
24. Wood, S., (2006) *Generalized Additive Models: An Introduction With R*, Chapman and Hall/CRC Press.
25. Zhao, H., Xiao, P., Feng, X. (2013) Edge Detection of Street Trees in High-Resolution Remote Sensing Images Using Spectrum Features. In Zhang, T., Sang, N., *MIPPR 2013: Automatic Target Recognition and Navigation*. Proceedings of SPIE 8918 AR UNSP 89180M. DOI 10.1117/12.2031224.

©Published by The James Hutton Institute, 2017 on behalf of ClimateXChange

All rights reserved. No part of this publication may be reproduced, stored in a retrieval system, or transmitted in any form or by any means, electronic, mechanical, photocopying, recording or otherwise, without the prior written permission of the publishers. While every effort is made to ensure that the information given here is accurate, no legal responsibility is accepted for any errors, omissions or misleading statements. The views expressed in this paper represent those of the author(s) and do not necessarily represent those of the host institutions or funders.